Dynamics of the dissociative electron attachment in H_2O and D_2O: The A_1 resonance and axial recoil approximation[#]

N BHARGAVA RAM, VAIBHAV S PRABHUDESAI and E KRISHNAKUMAR*

Tata Institute of Fundamental Research, Homi Bhabha Road, Colaba, Mumbai 400 005, India
e-mail: ekkumar@tifr.res.in

Abstract. The dynamics of the formation and decay of negative ion resonance of A_1 symmetry at 8.5 eV electron energy in the dissociative electron attachment (DEA) process in H_2O and D_2O are investigated using the velocity slice imaging technique. While the highest energy hydride ions formed by DEA show angular distributions characteristic to the A_1 symmetry, those formed with low-kinetic energy show considerably different angular distributions indicating changes in the orientation of the dissociating bond due to bending mode vibrations. Our observations are quite different from the recently reported measurements, but consistent with the fully quantum calculations.

Keywords. Dissociative attachment; velocity slice imaging; A_1 resonance in water.

1. Introduction

The formation and decay of negative ion resonance in electron-molecule collisions has attracted a great deal of attention recently. It is now realized that the electron-molecule resonance is the most critical link in a long chain of events leading to radiation damage in biological systems, nanolithography and the final products in various processing plasmas. It also plays a crucial role in the terrestrial and other planetary atmospheres and is considered to be important in the formation of large molecules in interstellar space. The relevance of negative ion resonances in all these arises due to the various highly reactive species it produces from its decay. The autodetachment of the electron could leave the molecule in excited vibrational and/or electronic state while the dissociation of the resonant state could produce one or more neutral radicals and a stable negative ion fragment, all of which could be highly reactive. Thus negative ion resonances are gateways through which the energy of free electrons is transferred efficiently to form reactive products. More crucially, in many situations this could lead to reaction channels that were not possible otherwise. The dissociation of a molecule following electron attachment is called dissociative electron attachment (DEA).

The DEA process is characterized by complex dynamics involving both electronic and nuclear degrees of freedom. Hence, the theoretical calculations of this process have met with very limited success, even for diatomic molecules. The situation becomes far more complicated for polyatomic molecules. As a result, very few calculations exist on these systems, despite heightened interest in the DEA process in complex molecules. Water is one exception to this. A series of papers on DEA to water has recently appeared which give a fairly accurate picture of the dynamics of the process.[1–8] It may be noted that apart from being one of the simplest polyatomic molecules, water is important from its ubiquitous presence and its heightened importance in biology.

Though there have been several studies of electron scattering on water, reliable cross sections for DEA in water across all the three resonances have become available only recently.[9] The resonances appear in DEA cross sections in the H^- channel dominantly with peak positions at 6.5 eV, 8.5 eV and 11.8 eV, respectively. They are also seen in the O^- channel at about the same energies, but with relatively low cross sections. These three resonances in water have been identified as due to core (or valence) excited Feshbach resonances where a bound electron being promoted to the LUMO, which is an a_1 orbital from the b_1 (HOMO), a_1 (HOMO-1) and b_2 (HOMO-2) orbitals, respectively by the incoming electron, while it is being captured into the a_1 (LUMO) orbital. In each of these three cases, there is a hole in the lower orbital and two electrons in the LUMO of the neutral molecule. Depending on the orbital in which the hole is present, the resonances have B_1, A_1 and B_2

---

symmetry, respectively with increasing electron energy. The structure and dynamics of these resonances have been investigated using ion kinetic energy spectrometry and angular distribution measurements.[10] Recent developments in the ion momentum imaging technique have allowed the structure and dynamics of the negative ion resonances in water to be studied in greater detail. The results on the momentum distribution of H^- and O^- from the three resonances in water have been discussed previously.[11,12] These results have been consistent with previous measurements using conventional technique[10] and are also well explained by the recent calculations[5] as far as the 6.5 eV resonance (B_1 symmetry) is concerned. However, the understanding of the momentum distributions of the ions from the 8.5 eV resonance (A_1 symmetry) and 12 eV resonance (B_2 symmetry) have been far from clear.[12] The recent experimental and theoretical results on the A_1 resonance in H_2O indicated the possibility of deviation from axial recoil approximation.[13] Axial recoil approximation implies that the molecule dissociates before any change in the initial orientation of the dissociating bond occurs due to rotation or any structural change. However, the accuracy of the results and the exact theoretical model needed to explain them has been debated[14,15] based on the momentum distribution of ions from H_2O. The purpose of this communication is to discuss the issues involved and try to settle the ambiguities based on the results from both H_2O and D_2O.

2. Experiment

The momentum distributions of the negative ions were measured using a Velocity Slice Imaging (VSI) technique, details of which have been reported earlier.[16] However, we present here a short description. The VSI is an improved version of the Velocity Map Imaging (VMI) technique.[17] In the VMI the Newton sphere of ions formed in a finite volume in the interaction region are extracted and focussed on to a two-dimensional position sensitive detector kept at the end of the specially designed time of flight spectrometer, in such a way that ions of a given velocity arrive at a given point on the detector within a narrow time spread irrespective of their point of formation in the interaction volume. Since in the conventional VMI no record of the time of arrival of the ions is kept, the recorded image is an integrated signal of the sphere along the time of flight axis. Because of the cylindrical symmetry about the electron beam, as in the present case or about the polarization direction in the case of photodissociation,

all the relevant information about the momentum distribution of the fragments are contained in any central slice of the Newton sphere containing the electron beam or the polarization vector as the case may be. The information of this central slice could be obtained from the integrated Newton sphere image by making use of an appropriate inversion algorithm like Abel inversion. In the present VSI experiment we stretch the Newton sphere along the flight tube axis while maintaining the VMI condition. Moreover, we record the position and time of arrival of each ion separately using a LIST mode data acquisition system.[18,19] The information on the central slice of the Newton sphere could be obtained in real time during data collection or later by selecting the appropriate time window, without using any of the inversion algorithms.

A schematic of the experiment is given in figure 1. In this experiment, a pulsed electron beam is allowed to interact with an effusive molecular beam at room temperature at right angle. The electron beam is pulsed with a repetition rate of 10 KHz and a width of 100 ns. A magnetic field of 50 gauss produced by a pair of Helmholtz coils kept outside the vacuum chamber, which encloses the VSI spectrometer is used to collimate the electron beam. The negative ions produced are extracted into the flight tube of the VSI spectrometer using a pulsed electric field. This pulse is applied with a delay of about 50 ns after the electron beam has left the interaction region, so that the low energy electron beam is not affected by the ion extraction field. The delayed extraction coupled with the finite width of the electron beam allows the blooming of the ion distribution in the interaction region before they are extracted. This leads to stretching of the Newton sphere allowing reliable velocity slice imaging. The extracted ions are focussed by a lens before they enter the flight tube.
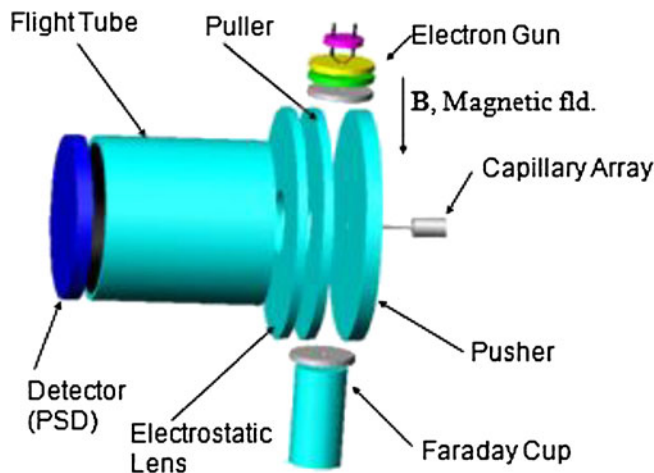

Figure 1. Schematic of the experimental arrangement.

The ions are detected using a two dimensional position sensitive detector made of three 50 mm diameter microchannel plates in Z-stack configuration followed by a Wedge and Strip anode. The position and time information from the detector corresponding to each ion striking it are recoded using a Camac based data acquisition system running on LAMPS.[18,19] LAMPS also allows analysis of the data during the experiment or at a later time.

3. Angular distribution under the axial recoil approximation

One of the important parameter that helps in identifying the structure of the resonance is the angular distribution of the fragment ions. The molecules are oriented equally in all directions in gas phase. However, when an electron interacts with a molecule, the probability for it to be resonantly captured is not the same in all directions. There are preferred orientations along which the probability of capture is maximum which depends on the symmetries of the neutral molecule and the negative ion resonance. Generally, the Born–Oppenheimer approximation is valid during the electron capture process and hence the nuclear co-ordinates of the resonant state would be the same as that of the neutral molecule right after the electron attachment process. If the dissociation of the negative ion resonance takes place before the molecule could rotate or undergo any structural changes, the angular distribution of the fragment negative ion retains the information on the orientation dependence of the electron capture process. This is called the axial recoil approximation. From the knowledge of the symmetry of the neutral molecule and the angular distribution of the fragment ion, one could retrieve information about the symmetry of the negative ion resonance under this approximation. A generic expression for the angular distribution for fragment ion from a diatomic molecule under axial recoil approximation has been given by O'Malley and Taylor[20] as

$$\frac{d\sigma}{d\Omega}(\Omega)$$
$$= \frac{4\pi^3}{k_i^2} \exp(-\rho_{Jr}) g \sum_{\Lambda_r} \left| \sum_{l=|\mu|}^{\infty} \langle \chi_{Jr} | V_{l|\mu|} | \chi_v \rangle Y_{l\mu}^*(\Omega) \right|^2,$$
(1)

in which χ_{Jr} and χ_v are vibrational wave functions of the resonance and the target molecule, respectively, g is the spin weighting factor, $\exp(-\rho_{Jr})$ is survival probability factor against autodetachment, $V_{l|\mu|}$ is the electronic transition matrix element and k_i is the incident electron momentum. Because of the conservation of the electronic axial orbital momentum there is a selection rule

$$\mu = \Lambda_f - |\Lambda_i|,$$
(2)

where Λ_i and Λ_f are the electronic axial orbital angular momenta of target state and resonant state, respectively. Tronc *et al.*,[21] have shown that under pure resonant scattering (PRS) approximation the term $< \chi_{Jr} | V_{l|\mu|} | \chi_v >$ can be written as $i^l a_{l|\mu|}$; where $a_{l|\mu|}$ is a real co-efficient. If a spherically symmetric potential scattering is included (PRS-PS approximation) the $< \chi_{Jr} | V_{l|\mu|} | \chi_v >$ term becomes $i^l \exp(i\delta_l) a_{l|\mu|}$ where δ_l is the potential scattering phase shift. Hence, for the case of only one resonant state contributing to the electron capture process, the angular dependence of the fragment anion in the case of diatomic molecule takes the general form

$$I(\theta, \phi, \varepsilon) \sim \left| \sum_{l=|\mu|}^{\infty} a_{l,|\mu|} Y_{l\mu}(\theta, \phi) \right|^2.$$
(3)

The l values are restricted by

$$l \geq |\mu|.$$
(4)

Notice that, in DEA, the extra electron carries one-half unit of spin, thus there exist inherent spin selection rule

$$S_f = S_i \pm 1/2.$$
(5)

With the same assumption i.e., only one resonance contributes at a time and the coupling is purely electronic type and the dissociation takes place faster than the rotation of the molecule, Azria *et al.*[22] have adopted the similar treatment for polyatomic molecules. For both diatomic and polyatomic molecules, assuming pure electronic coupling, the angular dependence is given by the matrix element $<\Phi_r | H_e | \Phi_{kiEi} >$ in which Φ_r is the resonant wavefunction, H_e is the electronic Hamiltonian, and Φ_{kiEi} is the initial wavefunction. The angular dependence comes from the fact that Φ_{kiEi} contains the incident plane wave $\exp(ik_i.r_e)$. For diatomic molecules this plane wave can be obtained from spherical harmonics, but in the case of polyatomic molecules, in order to determine the angular distribution, $\exp(ik_i.r_e)$ is expanded in linear combinations of spherical harmonics, which form a basis for the irreducible representations of the point group G of the molecule. These functions are denoted by Φ_{lm}^{γ} (with $m > 0$ and $\gamma = \pm 1$) and are chosen real. Then one can write:

$$\exp(ik_i \cdot r_e) = 4\pi \sum_{l=0}^{\infty} \sum_{m=0}^{l} i^l j_l(k_i, r_e) \sum_{\gamma=\pm 1} \Phi_{lm}^{\gamma*}(\hat{r}_e) \Phi_{l\mu}^{\gamma*}(\hat{k}_i).$$
(6)

This leads to the expression for the differential cross section to be

$$\frac{d\sigma}{d\Omega}(\hat{k}_i) \propto \left|\langle \Phi_r \,|H_e|\, \Phi_{\hat{k}_i E_i}\rangle\right|^2$$

$$\propto \left|\sum_{l,m,\gamma}' i^l \exp{(i\delta_l)}\, a_{lm}^{\gamma*}\Phi_{lm}^{\gamma*}(\hat{k}_i)\right|^2, \qquad (7)$$

in which δ_l is zero in PRS approximation. Also,

$$a_{lm}^{\gamma} = \int dr\, \Phi_r^* H_e \Phi_i\, j_l\,(k_i r_e)\, \Phi_{lm}^{\gamma}(\hat{r}_e), \qquad (8)$$

where a_{lm}^{γ} is real and equal to zero if Φ_{lm}^{γ} is not a basis for the irreducible representation $\Gamma_r X \Gamma_i$; Γ_r and Γ_i being the irreducible representations of the resonant and the target states, respectively. This selection rule leads to limit the sum in to the allowed values of l (Σ' indicates this limitation).

The equation 7 represents the dependence of the cross section on the orientation of k_i in the molecular frame. However, one wants the dependence of the cross section on the angle θ between the direction of dissociation and k_i. By using the rotation matrices one can transform the functions $\Phi_{lm}^{\gamma}\left(\hat{k}_i\right)$ into the functions $X_{lm}^{\gamma}(\theta, \phi)$ where (θ, ϕ) are the polar angles of k_i in the dissociation frame (in which the z axis has the direction of the bond that breaks). By averaging over the angle ϕ we obtain the following expression for the angular distribution in the laboratory frame:

$$I(\theta) \propto \frac{1}{2\pi}\int\limits_0^{2\pi} \frac{d\sigma}{d\Omega}(\theta, \phi)\, d\phi$$

$$\propto \frac{1}{2\pi}\int\limits_0^{2\pi} \left|\sum_{l,m,\gamma}' i^l \exp{(i\delta_l)}\, a_{lm}^{\gamma} X_{lm}^{\gamma*}(\theta, \phi)\right|^2 d\phi. \tag{9}$$

For attachment involving a given resonance, the expected angular distribution is a combination of the partial distributions for each allowed value of l. The general shape is, however, given by a linear combination of these partial distributions with coefficients $\left(a_{lm}^{\gamma}\right)^2$. The observed angular distribution of anion in DEA is fitted with spherical harmonics and the contributing spherical harmonics are determined by the symmetry of the transient molecular negative ion.

Water has C_{2v} symmetry with the ground electronic state being $^1A_1$. The procedure discussed above was used to obtain the scattering amplitude for a particular dissociation along a given bond for a given partial wave for a given symmetry of the negative ion resonance. The integration over ϕ was then used to get the corresponding angular distribution. Where more than one partial wave is expected to contribute, the integration was done after summing the individual amplitudes as given by equation 9. The final expressions for various resonances from molecules of different symmetries including that of water were then worked out.[23] It may be pointed out that exact calculations of the electron capture probability distribution as a function of the orientation of the molecule with respect to the electron beam for the three resonances in water have been reported recently by Adaniya *et al.*[13]

4. Results and discussion

The momentum images of H^- from H_2O with D^- from D_2O are shown in figure 2 at incident electron energies of 8.5 eV and 9.5 eV, respectively across the A_1 resonance. The images show maximum intensity in the 90° direction with respect to the electron beam. They also show that the ions are produced with a distribution of kinetic energies as evidenced by the distribution of intensity in the radial direction. The kinetic energy distributions of the ions integrated over all angles from the momentum images are shown in figure 3 in terms of the total kinetic energy release (KER) after taking into account the kinematic factors for electron energies of 8.5 eV and 9.5 eV, respectively. The KERs appear to be distributed from zero to a maximum energy allowed by the threshold energy for dissociation into the hydride ion and the hydroxyl radical (4.35 eV) and the electron energy. The slight extend of the energy distribution beyond what is allowed by the nominal electron energy is due to the high energy tail in the electron beam, as well as due to finite imaging resolution. This KER distribution corresponds to partition of energy into the kinetic energy and ro-vibrational excitation of the OH radical. It is seen that the KER in the case of H_2O is shifted to higher energies relative to that of D_2O. We also note some variation in this difference with respect to electron energy. The difference in the KER distribution between H_2O and D_2O could be explained in terms of a faster dissociation process in H_2O as compared to that of D_2O due to the difference in the reduced mass of the dissociating moieties in the two cases. The faster dissociation allows less energy to be transferred into the internal energy of the OH fragment through intramolecular vibrational redistribution (IVR) and hence the larger kinetic energy. The peak intensity in the 90° direction as seen in the images is not what is expected for the A_1 resonance under axial
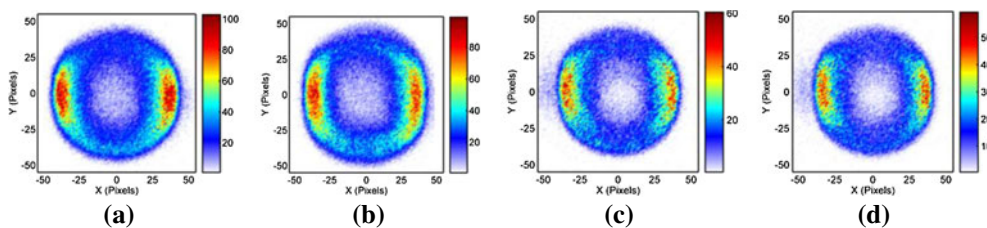
Figure 2. Velocity slice images of H$^-$ from H$_2$O at 8.5 eV (**a**) and 9.5 eV (**b**) and that from D$^-$ from D$_2$O at 8.5 eV (**c**) and 9.5 eV (**d**). The electron beam is in the plane of the figure directed vertically down.

recoil approximation. An exact calculation of the electron attachment probability at the equilibrium geometry of the neutral water molecule for the A$_1$ resonance as a function of polar angles about the centre of mass[13] also show that the peak intensity of the H$^-$ and D$^-$ angular distribution should be around 52° and 128°, respectively and not at 90° with respect to the electron beam direction. However, a detailed analysis shows that the angular distribution is a function of the ion kinetic energy. In figure 4 we present the angular distribution of the ions normalized at 90° for various kinetic energies. It may be noted that the kinetic energy and KER differ by about 5% in the case of H$_2$O and 10% in the case of D$_2$O. These are small in the context of the qualitative inferences we are making from the data.

The angular distributions given in figure 4 clearly show the higher kinetic energy ions have a different distribution as compared to that of lower energy ions. As mentioned earlier, the formation of higher energy ions indicate less energy being transferred to the OH radical through IVR before the dissociation occurs. This will correspond to almost instantaneous dissociation. Hence the corresponding angular distribution is expected to be closer to what is expected from the axial recoil approximation and hence closer to the true representation of

the orientation dependence of electron capture process. As seen from figure 4a and b, H$^-$ with larger kinetic energies (close to 4 eV; OH in ground vibrational state) show peaks at about 50° and 130°, respectively whereas those with lower kinetic energies (OH in higher vibrational states) peak at 90°. It is also seen that for the high energy ions the peak contrast increases with the kinetic energy. We also note that the peaks are more intense at the electron energy of 9.5 eV, as compared to those for 8.5 eV. It also appears that for the high kinetic energy ions (above 3 eV) there is considerably more intensity in the forward hemisphere as compared to the backward hemisphere. The intensity of ions of lower kinetic energy (below 3 eV) appears to peak at 90°. While the ones between 2 and 3 eV appear to have a symmetric distribution about 90°, those with energy less than 2 eV appear to have an asymmetry favouring the backward hemisphere, with the asymmetry increasing with reduction in kinetic energy. These details seen in the H$^-$ angular distribution appear to be present in the case of D$^-$ as well, as could be seen in figure 4c and d. On the whole, it appears that the high KER dissociation in both H$_2$O and D$_2$O following electron attachment forming the A$_1$ resonance follow axial recoil approximation fairly well, while the low KER dissociation show
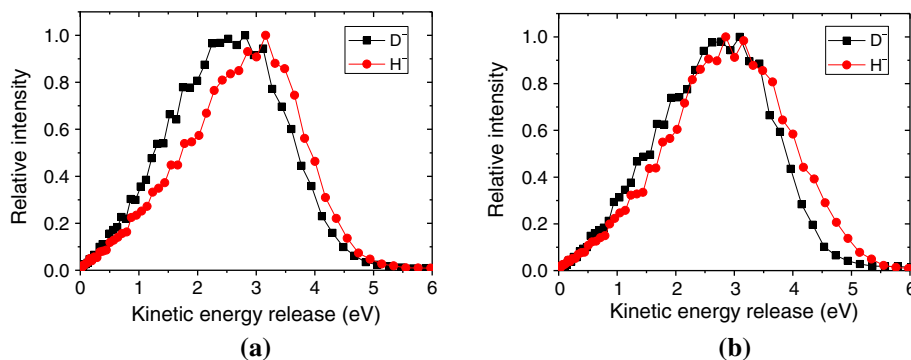

Figure 3. Kinetic energy release distribution of H$^-$ from H$_2$O (circles) and D$^-$ from D$_2$O (squares) at incident electron energy of 8.5 eV (**a**) and 9.5 eV (**b**). The data shown are obtained after integrating over entire 2π angles about the electron beam direction.
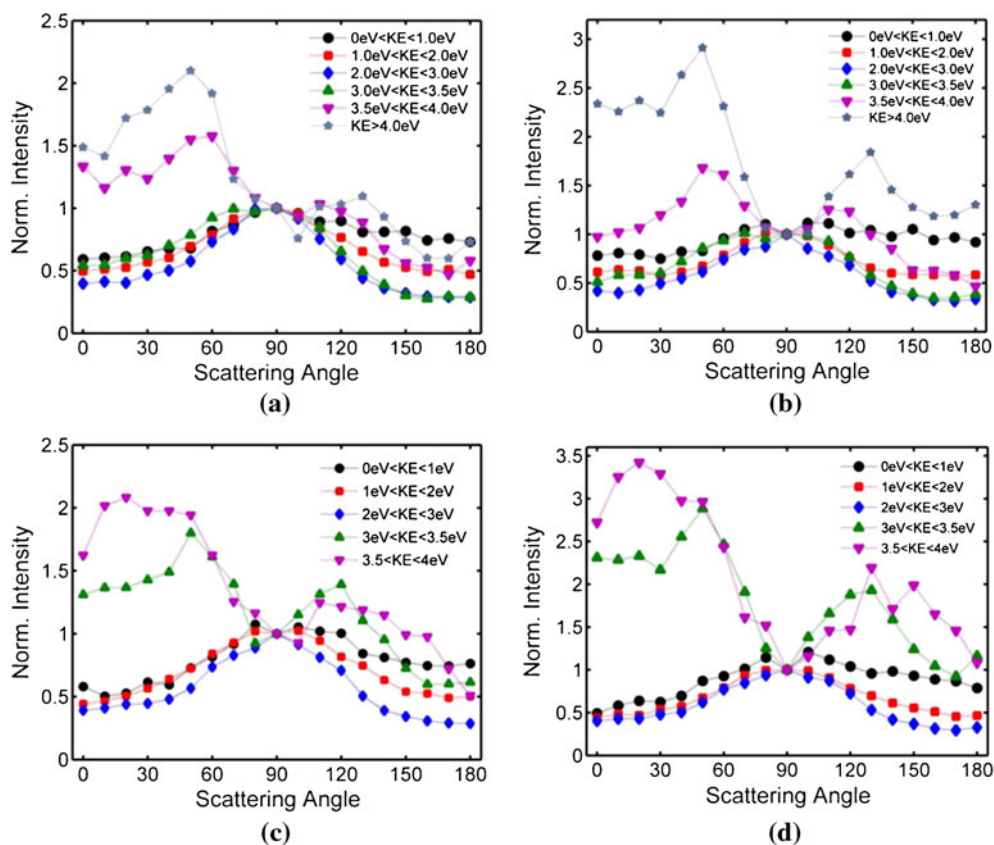
Figure 4. Angular distribution (normalized at 90°) of H^- from H_2O at incident electron energies of 8.5 eV (**a**) and 9.5 eV (**b**) and that of D^- from D_2O at 8.5 eV (**c**) and 9.5 eV (**d**) as a function of ion kinetic energy (KE). Circles: KE < 1 eV, squares: KE between 1 and 2 eV, diamonds: KE between 2 and 3 eV, triangles: KE between 3 and 3.5 eV, inverted triangle: KE between 3.5 and 4 eV and stars: KE > 4 eV. These plots show variation in angular distribution as a function of kinetic energy suggesting structural changes of the water anion due to bending mode vibrations prior to dissociation.

considerable deviation from it. It may also be noted that our measurements are in qualitative agreement with those of Belic *et al.*,[10] who observed that the high kinetic energy H^- ions have angular distribution peaking at 30° and 150°, respectively, while the low energy ions peaked at about 90°. This they had incorrectly attributed to possible contamination from the 6.5 eV resonance, which has an angular distribution peaking at 100° and has relatively larger cross section.

Recent measurements by Adaniya *et al.*[13] using a technique that they claim to be variation of COLTRIMS but using the Abel inversion algorithms to generate the angular distributions, showed varying angular distributions for the H^- ions as a function of their kinetic energy. For ions of kinetic energy near 4 eV they found the angular distribution to be peaking at 40° and 100°, respectively with larger intensity in the backward hemisphere. This is distinctly different from what we observe. However, the angular distribution for ions with kinetic energy near 2 eV was found to be somewhat

similar to what we observe. The difference in the angular distribution for high energy ions as observed by Adaniya *et al.* could be due to poor momentum resolution that they have for large kinetic energy ions. This could be seen from their reported kinetic energy release data, which appeared to extend well beyond what is physically possible for the electron energy used. It may be noted that while we use the Velocity Slice Imaging to obtain the momentum images directly, Adaniya *et al.* used a reconstruction algorithm to obtain the momentum images from the integrated Newton sphere. The inversion procedure also may have contributed to some inaccuracies in their final results.

As mentioned earlier, Adaniya *et al.*[13] also carried out fully quantum calculations of the electron attachment probability as a function of the polar angles about the centre of mass. From these results one can obtain the expected angular distribution of the fragment ions under axial recoil approximation. As their experimental results did not agree with these calculations, they

tried to explain it in terms of deviation from axial recoil approximation. This is caused due to the structural changes that H_2O^{-*} molecular negative ion undergoes due to bending mode vibrations before the dissociation could take place, thereby distorting the angular distributions. Their classical trajectory calculations using the potential energy surfaces constructed for 2A′ state showed that the H–O–H bond angle opens up quickly following electron attachment and the hydrogen recoil axis reorients it towards and beyond linear geometry at 90°. They also found that the trajectories in which one of the H atoms takes more of the available kinetic energy undergoes less bending motion before dissociation. However, these classical trajectory calculations did not show the desired agreement with their experimental data on ions of high KER due to possible errors in their experimental technique as pointed out earlier.

We fit the angular distribution of ions with 4 eV for A_1 symmetry using the lowest order partial waves as shown in figure 5. Fits for H^- from H_2O and D^- from

D_2O at electron energies of 8.5 eV and 9.5 eV, respectively are given. The relative partial wave contributions and the corresponding phase shifts are given in table 1. We note that good fits could be obtained only after including the d-wave contribution. The fits using only the s- and p-waves do not reproduce the peaks. Also, unrealistically large amplitudes of p-wave with respect to that of s-wave are obtained at least in three cases, indicating the need for inclusion of the d-wave. The table also shows that d-wave provides the dominant contribution. It may be noted that in order to reproduce the results of the fully quantum calculations of Adaniya *et al.*[13] under axial recoil approximation, considerable contribution from the d-wave is essential. In figure 6 we compare the angular distribution of H^- ions of 2 eV kinetic energy obtained at electron energy of 8.5 eV with the results of the classical trajectory calculations of Adaniya *et al.* which took into account the bending mode vibration of the molecule before dissociation. We note that the calculation agree with our measurements fairly well. Here again, our results are more consistent
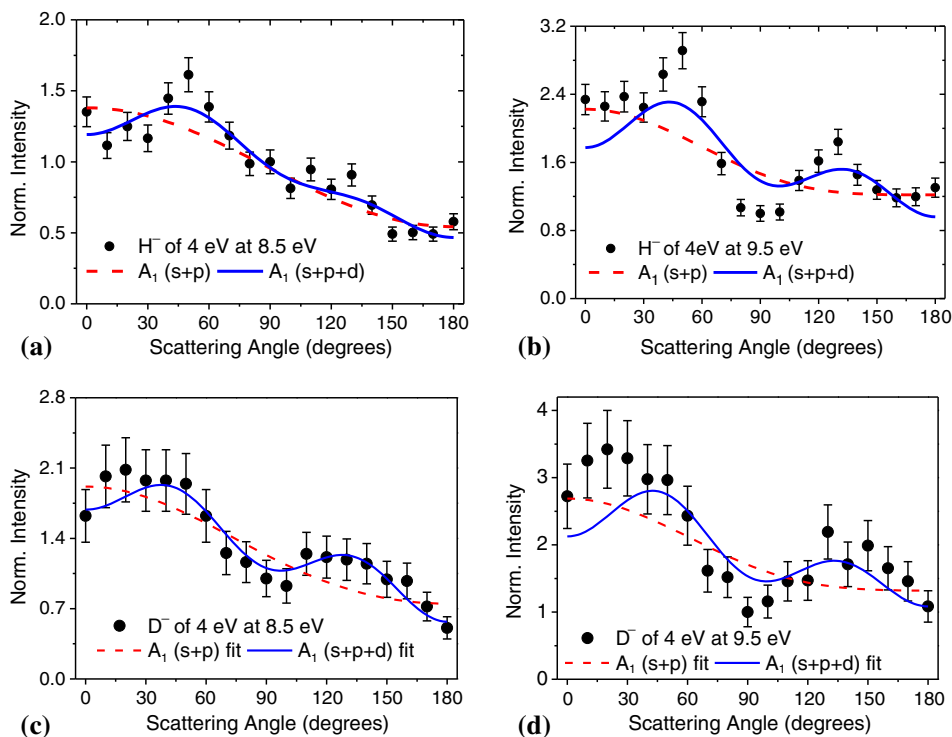

Figure 5. Fits of the angular distribution of H^- and D^- ions assuming A_1 symmetry for the resonance under axial recoil approximation. The plots are for H^- ions of KE 4 eV at incident electron energy of 8.5 eV (**a**) and 9.5 eV (**b**) and D^- ions of KE 4 eV at incident electron energy of 8.5 eV (**c**) and 9.5 eV (**d**). All the data are normalized to that at 90°. Circles: measured intensity, dashed lines: fits for A_1 symmetry with *s* and *p* partial waves, and solid lines: fits for A_1 symmetry with *s*, *p* and *d* partial waves. The relative amplitudes and phases obtained from the fits are given in table 1.

Table 1. Relative amplitudes and phase shifts obtained by fitting partial wave contributions to the angular distribution for A_1 symmetry at electron energies of 8.5 eV and 9.5 eV, respectively for hydride ions of kinetic energy 4 eV from H_2O and D_2O.

Ion	Electron energy (eV)	Relative amplitudes			Relative phase shift (radians)	
		s-wave	p-wave	d-wave	δ_{sp}	δ_{sd}
H^-	8.5	1	0.35	-	~ 0	-
H^-	8.5	1	0.85	1.12	1.07	2.29
H^-	9.5	1	9.81	-	~ 0	-
H^-	9.5	1	0.3	1.33	0	0
D^-	8.5	1	3.6	-	1.02	
D^-	8.5	1	0.47	1.29	0	1.53
D^-	9.5	1	8.55	-	0	-
D^-	9.5	1	0.31	1.1	0	0

with possible deviation from axial recoil approximation as seen by the better agreement with the classical trajectory calculation than the experimental results of Adaniya *et al.*[13]

5. Conclusion

The momentum images of H^- from H_2O and D^- from D_2O across the A_1 resonance show clear evidence of the deviation from axial recoil approximation. This deviation is found to be a function of the KER of the dissociation process. While the angular distribution of the ions corresponding to the highest possible KER appears to follow the axial recoil approximation indicating very little change in the molecular geometry or bond orientation before dissection, that of low energy ions shows strong deviation from the axial recoil

approximation. The angular distribution of the low energy ions show that the orientation of the O–H (O–D) bond has undergone a change before dissociation took place. We find that these observations are consistent with a model in which the molecule undergoes bending mode vibrations before the dissociation could take place. The angular distribution of the high energy ions appear to be consistent with the recent fully quantum calculations. We also note strong d-wave contribution in the attachment process based on the fit for A_1 symmetry.

References

1. Gorfinkiel D, Morgan L A and Tennyson J 2002 *J. Phys. B: At. Mol. Opt. Phys.* **35** 543
2. Haxton D J, Zhang Z, McCurdy C W and Rescigno T N 2004 *Phys. Rev. A* **69** 62713
3. Haxton D J, Zhang Z, Meyer H-D, Rescigno T N and McCurdy C W 2004 *Phys. Rev. A* **69** 062714
4. Haxton D J, Rescigno T N and McCurdy C W 2005 *Phys. Rev. A* **72** 022705
5. Haxton D J, McCurdy C W and Rescigno T N 2006 *Phys. Rev. A* **73** 062724
6. Haxton D J, McCurdy C W and Rescigno T N 2007 *Phys. Rev. A* **75** 012710
7. Haxton D J, Rescigno T N and McCurdy C W 2007 *Phys. Rev. A* **75** 012711
8. Haxton D J, Rescigno T N and McCurdy C W 2008 *Phys. Rev. A* **78** 040702(R)
9. Rawat P, Prabhudesai V S, Aravind G, Rahman M A and Krishnakumar E 2007 *J. Phys. B: At. Mol. Opt. Phys.* **40** 4625
10. Belic D S, Landau M and Hall R I 1981 *J. Phys. B: At. Mol. Phys.* **14** 175
11. Bhargava Ram N, Prabhudesai V S, Aravind G, Rawat P and Krishnakumar E 2007 *J. Phys. Conference Series* **80** 012017
12. Bhargava Ram N, Prabhudesai V S and Krishnakumar E 2009 *J. Phys. B: At. Mol. Opt. Phys.* **42** 225203
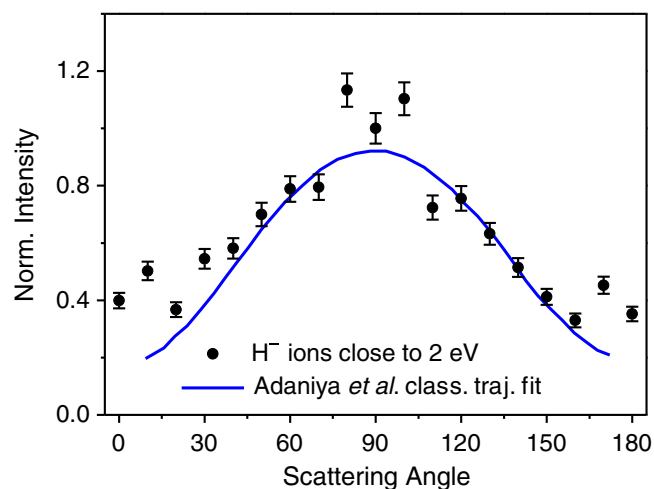
Figure 6. Angular distribution of H^- ions with kinetic energy of 2 eV at 8.5 eV electron energy (circles) and comparison with classical trajectory calculations of Adaniya *et al.*[13] (solid line).

13. Adaniya H, Rudek B, Osipov T, Haxton D J, Weber T, Rescigno T N, McCurdy C W and Belkacem A 2009 *Phys. Rev. Lett.* **103** 233201
14. Ram N B, Prabhudesai V S and Krishnakumar E 2011 *Phys. Rev. Lett.* **106** 049301
15. Adaniya H, Rudek B, Osipov T, Haxton D J, Weber T, Rescigno T N, McCurdy C W and Belkacem A 2011 *Phys. Rev. Lett.* **106** 049302
16. Nandi D, Prabhudesai V S, Chatterjee A and Krishnakumar E 2005 *Rev. Sci. Instrum.* **76** 053107
17. Eppink A and Parker D H 1997 *Rev. Sci. Instrum.* **68** 3477
18. Chatterjee A http://www.tifr.res.in/~pell/lamps.html
19. Chatterjee A, Kamerkar S, Jethra A K, Padmini S, Diwakar M P, Pande S S and Ghodgaonkar M D 2001 *Pramana, J. Phys.* **57** 135
20. O'Malley T F and Taylor H S 1968 *Phys. Rev.* **176** 207
21. Tronc M, Fiquet-Fayard F, Schermann C and Hall R I 1977 *J. Phys. E: At. Mol. Phys.* **10** 305
22. Azria R, Le Coat Y, Lefevre G and Simon D 1979 *J. Phys. B: At. Mol. Phys.* **12** 679
23. Ram N B 2010 *Dissociation dynamics in polyatomic molecules due to electron attachment*. Ph. D. Thesis, Tata Inst. of Fundamental Research, Mumbai